



Article

Engineering the C3N Pathway as a Short Detour for *De Novo* NAD⁺ Biosynthesis in *Saccharomyces cerevisiae*

Xinli Li ^{1,2,†}, Yue Tang ¹, Yong Ding ¹, Pengwei Li ^{1,*}  and Yihua Chen ^{1,2,*} 

¹ State Key Laboratory of Microbial Resources, Institute of Microbiology, Chinese Academy of Sciences, Beijing 100101, China; lixinli_1@sina.com (X.L.); tangy@im.ac.cn (Y.T.); dingyong14@mailsucas.ac.cn (Y.D.)
² University of Chinese Academy of Sciences, Beijing 100049, China
* Correspondence: lipw@im.ac.cn (P.L.); cheniyihua@im.ac.cn (Y.C.)
† Current address: Department of Physiology, Faculty of Basic Medical Sciences, Hubei University of Medicine, Shiyan 442000, China.

Abstract: As a life-essential coenzyme, nicotinamide adenine dinucleotide (NAD⁺) has been explored for more than a century. In *Saccharomyces*, the natural NAD⁺ *de novo* biosynthetic pathway initiating from tryptophan has been well elucidated. To bypass this stringently controlled natural pathway in yeast, an economical C3N pathway that was developed in *Escherichia coli* previously was constructed in *Saccharomyces* as a short detour for *de novo* NAD⁺ biosynthesis. After the functional expressions of the C3N genes were identified in *Saccharomyces cerevisiae* BY4741 by in vitro enzymatic assays, the C3N module was introduced into an NAD⁺ auxotrophic *S. cerevisiae* strain BY01, in which the *BNA2* gene encoding tryptophan 2,3-dioxygenase was inactivated. The efficient NAD⁺ synthesis via the C3N pathway was confirmed by both plate assays and fermentation analysis. The applicability of the C3N pathway in cofactor engineering was tested by introducing it into *S. cerevisiae* BY4741, which improved the cellular NAD(H) level considerably. Consequently, this study proved that the *de novo* NAD⁺ biosynthetic pathway can be replaced by an artificial pathway in yeast, which paves a way to design more promising schemes in eukaryotes for rational manipulation of the cellular NAD(H) levels.

Keywords: C3N pathway; NAD⁺ *de novo* biosynthesis; *Saccharomyces cerevisiae*; eukaryotes



Citation: Li, X.; Tang, Y.; Ding, Y.; Li, P.; Chen, Y. Engineering the C3N Pathway as a Short Detour for *De Novo* NAD⁺ Biosynthesis in *Saccharomyces cerevisiae*. *Fermentation* **2023**, *9*, 886. <https://doi.org/10.3390/fermentation9100886>

Academic Editors: Guoqiang Zhang and Jianghua Li

Received: 11 September 2023
Revised: 27 September 2023
Accepted: 28 September 2023
Published: 29 September 2023



Copyright: © 2023 by the authors. Licensee MDPI, Basel, Switzerland. This article is an open access article distributed under the terms and conditions of the Creative Commons Attribution (CC BY) license (<https://creativecommons.org/licenses/by/4.0/>).

1. Introduction

Nicotinamide adenine dinucleotide (NAD⁺) and its reduced form NADH predominately function as electronic donor and acceptor in more than a quarter of the cellular redox reactions [1]. In addition, NAD⁺ is a substrate of many NAD⁺-consuming enzymes, which play essential roles in signal transduction pathways regulating crucial biological processes, e.g., DNA repair, transcription, and cell cycle progression [2]. Apart from the important physiological functions of NAD⁺, a common cognition about NAD⁺ was its cellular supply. Engineering to modulate the cellular concentration of NAD(H) is a practical way to tune the catalytic efficiencies of NAD(H)-dependent and NAD⁺-consuming enzymes, which has been performed not only for research purposes in prokaryotic and eukaryotic cells but also for valuable products bio-manufacturing in industry [3,4]. Several different strategies have been developed to modulate cellular NAD(H) levels, including supplementation of NAD⁺ or its precursors, reduction of NAD⁺ consumption, and reinforcement of NAD⁺ biosynthesis pathways [5,6]. The efficiency of the last strategy has been proven in many cases; people can expand the cellular NAD(H) pools and accelerate its replenishment by strengthening the *de novo* biosynthesis pathway, as well as the salvage pathway of NAD⁺ [7,8].

To date, only two natural *de novo* NAD⁺ biosynthesis pathways have been delineated [4,9]. Pathway I, which distributes in plants and most bacteria, uses L-aspartate (L-Asp) as a precursor for the nicotinamide moiety of NAD⁺ [10,11], whereas pathway II, which exists in some bacteria, mammals, and fungi, recruits L-tryptophan

(L-Trp) as a precursor [4,12]. The *de novo* biosynthesis pathways of NAD⁺ are essential to cells in most cases and are tightly controlled at transcriptional, translational, and post-translational levels [13–15], which may explain the difficulties in modulating cellular NAD(H) levels by engineering on those pathways. Recently, we constructed an alternative *de novo* NAD⁺ biosynthesis pathway in *Escherichia coli*, the C3N pathway, which uses chorismate as a starter unit and converts it to 3-hydroxyanthranilic acid (3-HAA) by three enzymes, PhzD, PhzE, and DhbX, from secondary metabolism [16]. Subsequently, 3-HAA is converted to quinolinic acid (QA) by 3-HAA 3,4-dioxygenase, which is also a key enzyme in pathway II for NAD⁺ synthesis [17]. The three steps from QA to NAD⁺ are conserved for all *de novo* biosynthesis pathways of NAD⁺ [9]. The newly developed C3N pathway circumvents the stringent regulation on *de novo* NAD⁺ biosynthesis and results in a more than nine times improvement of the cellular NAD(H) level in *E. coli*, demonstrating its powerfulness in cofactor engineering [16]. However, all enzymes used for constructing the C3N pathway in *E. coli* are of bacterial origins; the applicability of this pathway in eukaryotic cells remains to be exploited.

As a classical representative of eukaryotic cells, *Saccharomyces cerevisiae* is a generally recognized as safe (GRAS) industrialized cell for the production of valuable chemicals, such as food additives, natural products, and pharmaceutical precursors [18]. It is also an ideal molecular biology model for the study of NAD⁺-dependent physiological processes such as aging and related diseases and signaling pathways [19,20]. *S. cerevisiae* synthesizes NAD⁺ from L-Trp via *de novo* pathway II [21]. As depicted in Figure 1, L-Trp is converted to 3-HAA, the shared intermediate of pathway II and the C3N pathway, by four steps. Moreover, L-Trp is derived from chorismate by five enzymatic reactions. Therefore, it takes nine steps for the conversion of chorismate to 3-HAA during the native NAD⁺ biosynthesis in *S. cerevisiae*. The C3N pathway only needs three steps for the conversion of chorismate to 3-HAA, which is certainly an economical short detour for NAD⁺ biosynthesis. Actually, almost all reported successful cases about improving the cellular NAD(H) levels in *S. cerevisiae* are via manipulations on the salvage pathway instead of the *de novo* pathway, which may reveal the difficulty in modulating the tightly controlled pathway II for cofactor engineering [21]. The artificial C3N pathway may circumvent the native regulation and serves as an alternative for expanding the cellular NAD(H) pool of *S. cerevisiae*. In addition, the C3N pathway decouples protein synthesis and NAD⁺ *de novo* biosynthesis by recruiting a non-proteinogenic amino acid precursor, which makes it suitable for biotransformation that needs protein overexpression.

In this work, we firstly verified that all three necessary bacterial genes (forming the C3N module) for the construction of C3N pathway could be functionally expressed in *S. cerevisiae*. An NAD⁺ auxotrophic *S. cerevisiae* strain that could survive on NAD⁺ synthesized solely by the C3N pathway was then constructed, revealing that the C3N pathway is also efficient in eukaryotes. When the C3N module was expressed in wild-type *S. cerevisiae*, a considerable increment of the cellular NAD(H) level was observed, demonstrating the applicable potential of the C3N module in cofactor engineering.

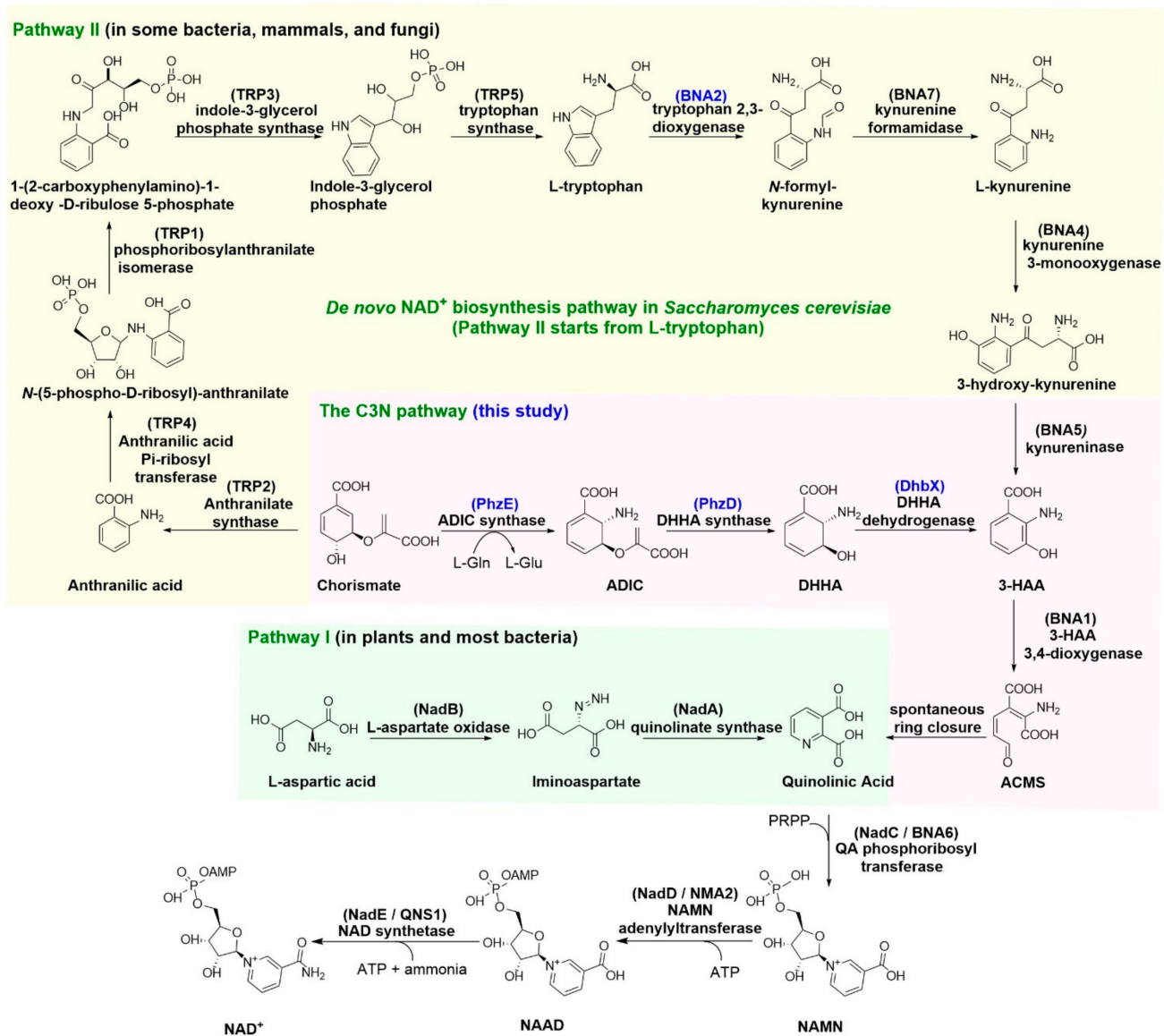


Figure 1. The three NAD⁺ *de novo* biosynthesis pathways. Enzymes used in this work are indicated with blue. ADIC: 2-amino-2-deoxyisochorismate; DHHA: trans-2,3-dihydro-3-hydroxyanthranilic acid; 3-HAA: 3-hydroxyanthranilate; ACMS: 2-amino-3-carboxymuconate semialdehyde; PRPP: 5-phosphoribosyl diphosphate; NAMN: nicotinic acid mononucleotide; NAAD: nicotinic acid adenine dinucleotide.

2. Materials and Methods

2.1. Strains, Plasmids, and Growth Conditions

Strains and plasmids used in this study were summarized in Table S1. *E. coli* JM109 was used for DNA cloning and propagation of plasmids. *S. cerevisiae* BY4741 was used for expressing recombinant proteins. LB medium (10 g/L peptone, 5 g/L yeast extract, and 10 g/L NaCl) with or without 20 g/L agar was used for the growth of *E. coli* strains and propagation of plasmids at 37 °C, and, if necessary, 100 µg/mL ampicillin and 50 µg/mL kanamycin were added. YPD medium (10 g/L yeast extract, 20 g/L peptone, and 20 g/L glucose), nicotinic acid drop-out YMM medium (YMMN medium) [22], and yeast nitrogen base supplemented with essential nutrients medium (YNB-S) (6.7 g/L Yeast nitrogen base without amino acids (#Y0626, Sigma, Beijing, China), 1.92 g/L Yeast Synthetic Drop-out Media Supplements (#Y1501, Sigma, Beijing, China), and 20 g/L glucose) with or without

20 g/L agar were used for growth of *S. cerevisiae* strains at 30 °C. If necessary, 150 mg/L uracil and/or 1 g/L 5-fluoroorotic acid were supplemented.

2.2. General DNA Manipulations and Sequence Analyses

DNA synthesis and sequencing were performed by Generay Biotech (Shanghai, China) and Genewiz (Suzhou, China), respectively. The classical lithium acetate/single-stranded carrier DNA/PEG method was used for *S. cerevisiae* genetic manipulation and plasmid transformation according to the standard protocols [23]. The chemical transformation method was used for *E. coli* transformation and plasmids propagation according to the standard protocols [24]. To construct the different engineered plasmids, the one-step cloning method was employed according to the manufacturer's instructions (Vazyme, Nanjing, China). PCRs were performed with the Q5 DNA polymerase (NEB, Beijing, China). The digestion of plasmids was carried out by restriction enzymes (Takara, Dalian, China) following the general methods [25].

2.3. Construction of *S. cerevisiae* BY01

To inactivate the tryptophan 2,3-dioxygenase gene *BNA2*, the about 0.5 kb upstream and downstream flanked fragments of *BNA2* were amplified with primers BNA2-U-F (TTTGCCCTCCAATTCCTAGGGATTGGCTAACGATGGTTGG)/BNA2-U-D (TGGCGTAATAGCGAAGAGGCCATCGGCGTTGACTCTTTCTT) and BNA2-D-F (CAAAAGCTGAGCTGGCCTTGTGATAGACGGGTTGGAGGGC)/ BNA2-D-D (CATCGTTAGCCAATCCTAGGGAATTGGAGGGCAAATAAT) from the *S. cerevisiae* BY4741 genome and inserted into the *Sfi*I site of pUMRI-21(A) to generate pRU-BNA-UD, which was then linearized by *Avr*II and introduced into *S. cerevisiae* BY4741. The transformants were spread on YNB-S plates without uracil and cultured at 30 °C for 3 days. One of the transformants was inoculated into 10 mL YPD medium and cultured at 30 °C, 220 rpm for 24 h. The cells of 200 µL culture were collected by centrifugation, washed twice with ddH₂O, and spread on YNB-S plates with 150 mg/L uracil and 1 g/L 5-fluoroorotic acid. After incubation at 30 °C for 3 days, one of the transformants was verified as BY01 by primers BNA2-F (GATTGGCTAACGATGGTTG)/BNA2-R (GAATTGGAGGGCAAATAAT).

2.4. Expression of *phzD*, *phzE*, and *dhbX* Individually in *S. cerevisiae*

To express *phzD* in *S. cerevisiae* BY4741, the codon-optimized *phzD* gene was synthesized and inserted into plasmid pYES2.0 to afford pYES2.0-*phzD*. The 0.4 kb *TEF1* promoter P_{TEF1} was cloned from the *S. cerevisiae* genome by primer pair TEF-DR (GCTTGGTACCGAGCTCGGATCGATCTTCAAATGTTTCTAC)/TEF1p-R (ATAGTGAGTCGTATTACGGATCCTAGAAAACCTTAGATTAGA) and was ligated with the 6.1 kb PCR fragment amplified with primer pairs Gal-OF (GAGCTCGGTACCAAGCTACTAGTGGATCATCCCCACG)/T7 (TAATACGACTCACTATAGG) using pYES2.0-*phzD* as a template to construct pYE- P_{TEF1} -*phzD*, in which the *GAL1* promoter P_{GAL1} was replaced by the promoter P_{TEF1} . *S. cerevisiae* BY00-*phzD* was then obtained by introducing pYE- P_{TEF1} -*phzD* into *S. cerevisiae* BY4741 by chemical transformation. As described above, constructions of *S. cerevisiae* BY00-*phzE* and BY00-*dhbX* were carried out using the same procedures. To express the proteins PhzD, PhzE, and DhbX individually in *S. cerevisiae*, the engineered strain was inoculated in YNB-S medium without uracil and cultured at 30 °C, 220 rpm for 48 h. The seeds culture was inoculated into YPD medium at 1% ratio (*v/v*) and cultured at 30 °C, 220 rpm for 24–36 h. The cells were harvested by centrifugation (4 °C, 3000× *g*, 20 min) and re-suspended in lysis buffer (20 mM Tris-HCl, 500 mM NaCl, 5 mM imidazole, pH 7.9) and burst by ultrasonication, and the cell debris was removed by centrifugation (4 °C, 16,000× *g*, 30 min). The crude proteins PhzD, PhzE, and DhbX were desalted and concentrated by ultrafiltration using a Millipore centrifugal filter (15 mL, 10 kD MWCO), respectively, and stored at −80 °C in HEPES buffer (pH 8.0, for PhzD and PhzE) and in PBS buffer (pH 7.4, for DhbX) with 20% glycerol [26], respectively.

Functions of those three proteins were verified by enzymatic assays using the crude proteins as catalysts. The PhzE activity was tested in a 50 μ L mixture containing 100 mM HEPES buffer (pH 8.0), 1 mM chorismate, 10 mM glutamine, 10 mM $MgCl_2$, and 20 μ L crude PhzE at 30 $^{\circ}C$ for 1 h; the PhzD activity was checked in a 50 μ L mixture containing 100 mM HEPES buffer (pH 8.0), 1 mM chorismate, 10 mM glutamine, 10 mM $MgCl_2$, 5 μ L crude PhzD, and 20 μ L crude PhzE at 30 $^{\circ}C$ for 1 h; the DhbX activity was detected in a 50 μ L mixture containing 50 mM PBS buffer (pH 7.4), 2 mM NAD^+ , 2 mM DHHA, and 10 μ M crude DhbX at 37 $^{\circ}C$ for 1 h. BY4741 with the empty pYES2.0 plasmid (designated as *S. cerevisiae* BY00-Con) was used as a control. The reactions were quenched with an equal volume of $CHCl_3$. After centrifugation, the aqueous phases of the reactions (10 μ L) were analyzed by HPLC.

2.5. Construction of *S. cerevisiae* BY00-Con, BY00-C3N, BY01-Con, and BY01-C3N

To construct *S. cerevisiae* BY01-C3N, the 0.6 kb *phzD* gene was PCR cloned from pYES2.0-*phzD* with primer pair *phzD*-F (ATGCATCATCATCATCATTCAGGTATTCCAG)/*phzD*-R (CGAAGAATTGTTAATTAAGAGCTCTTATTCCAAGACTTC) and inserted into the *SacI*/*EcoRI* sites of pUMRI-21(A) to generate pRU-ZD (Ga). The about 1.9 kb *phzE* gene was amplified from pYES2.0-*phzE* using primer pair *phzE*-F (CTCGAGTTAAGGTCTTCTTCAACCA)/*phzE*-R (GTAATACGACTCACTATAGGGTCGACATGCATCATCATCATCATATAACGC) and inserted into the *SalI*/*XhoI* sites of pRU-ZD (Ga) to generate pRU-ZDE (Ga). Then, the 0.4 kb *TEF1* promoter P_{TEF1} and 0.6 kb *PGK1* promoter P_{PGK1} were amplified using *S. cerevisiae* genome as a template with primer pair *TEF1P*-F (GTTTGCCCTACGTTTGGCATCTTCAAAATGTTTCTA)/*TEF1P*-R (ATAGTGAGTCGTATTACGGATCCTAGAAAAGTTAGATTAGA) and *PGK1*-F (GCAAAACGTAGGGG CA AACCCGATTGGGCGCGAATCC)/*PGK1*-R (GAATGATGATGATGATGATGCATTGTTT-TATATTTGTTGTA AAAAG), respectively. The two promoters were inserted upstream of *phzE* and *phzD* in pRU-ZD (Ga), respectively, using the one-step cloning method to generate pRU-ZDE (Co). The 4.2 kb cassette (T_{CYC1} -*phzE*- P_{TEF1} - P_{PGK1} -*phzD*- T_{TDH1}) was amplified from pRU-ZDE (Co) using primer pair *phzDE*-F (CGCGTGGGGATGATCCACTAGTAGC TTGGTACCCTTCGAGCGTC)/*phzDE*-R (CGATCCGAGCTCGGTACCGGCCTCTTCGC-TATTACGCC) and inserted into the *KpnI* site of pYE- P_{TEF1} -*dhbX* to generate pY-C3N. *S. cerevisiae* BY01-C3N and BY00-C3N were then obtained by introducing pY-C3N into *S. cerevisiae* BY01 and BY00, respectively. The control strain *S. cerevisiae* BY00-Con and BY01-Con was constructed by introducing empty pYES2.0 into *S. cerevisiae* BY00 and BY01, respectively.

2.6. Growth of *S. cerevisiae* Strains on YMMN Plates

The different *S. cerevisiae* strains were inoculated into 3 mL YNB-S medium (with or without 150 mg/L uracil) for 48 h. The seeds were inoculated into 10 mL YMMN medium (with or without 150 mg/L uracil) and cultured for 24 h. The cells were then collected by centrifugation and washed twice by ddH_2O . For the growth experiments on agar plate, 1.5 μ L dilutions (OD_{600} of 0.1) of different strains were spotted onto YMMN agar and grown at 30 $^{\circ}C$ with varied supplements. *S. cerevisiae* BY00 was spotted onto YMMN agar supplemented with 150 mg/L uracil; *S. cerevisiae* BY01 was inoculated onto YMMN agar (150 mg/L uracil) with or without 10 mM QA; *S. cerevisiae* BY01-Con was inoculated onto YMMN agar with or without 10 mM QA; and *S. cerevisiae* BY01-C3N was spotted onto YMMN agar directly.

2.7. Measurement of Intracellular NAD(H) Concentrations

The different *S. cerevisiae* strains were inoculated into 3 mL YNB-S medium (with or without 150 mg/L uracil) for seed growth under 30 $^{\circ}C$, 220 rpm for 48 h. The cells were collected by centrifugation, washed twice with ddH_2O , and resuspended into YMMN medium. Then, the growth condition of the engineering strains was first tested by test tube with 3 mL YMMN medium; subsequently, the different strains were cultured into

20 mL YMMN medium in a 100 mL shake flask at a final OD₆₀₀ of 0.02. The culture was grown at 30 °C, 220 rpm for 36 h. To measure the intracellular NAD(H) concentration, the cells were harvested by centrifugation (4 °C, 3000 × g, and 5 min) at the time point of four hours after entering the stationary phase. The cell pellets were washed with ice-cold PBS buffer, re-suspended in the same buffer, and adjusted to OD₆₀₀ of 1.0. The concentrations of NAD(H) (total NAD⁺ and NADH) and NAD⁺ only were measured by enzyme cycling-based colorimetric assay [27]. *S. cerevisiae* was calculated as 3×10^7 cells/mL at OD₆₀₀ of 1.0, and the volume of one *S. cerevisiae* cell was 70 μm³ [28,29]. The growth curve was supervised by Multi-mode Microplate Reader (Synergy H1, BioTek, Winooski, VT, USA) with an interval of 6 h.

2.8. Spectroscopic Analysis

HPLC analysis was performed with a ZORBAX SB-Aq Stable-Bond Analytical column (5 μm, 4.6 × 250 mm, Agilent Technologies, Santa Clara, CA, USA) on a Shimadzu HPLC system (Shimadzu, Kyoto, Japan) [30]. The column was developed with solvent A (water with 0.1% trifluoroacetic acid) and acetonitrile at a flow rate of 1 mL/min except for the DHHA dehydrogenase assays (0.8 mL/min). For analysis of the DHHA dehydrogenase reactions, the percentage of acetonitrile was changed linearly from 1% to 50% over 0–30 min, from 50% to 100% over 30–32 min, and maintained at 100% for 5 min; for analysis of the crude PhzD- and/or PhzE-containing enzymatic assays, the ratio of acetonitrile was changed linearly from 0% to 5% over 0–2 min, from 5% to 50% over 2–17 min, from 50% to 100% over 19–21 min, and maintained at 100% for 10 min. To detect the intermediates of NAD⁺ biosynthesis in *S. cerevisiae* strains, the ratio of acetonitrile was initially stayed 0% over 1 min, changed from 0% to 5% over 1–4 min, from 5% to 20% over 4–19 min, from 20% to 22% over 19–21 min, from 22% to 100% over 21–23 min, and maintained at 100% for 10 min. The detection wavelength of chorismate, ADIC, and DHHA was 280 nm, and it was 294 nm for 3-HAA analysis.

2.9. Sequence Data

The GenBank accession numbers of the original *phzE*, *phzD*, and *dhbX* genes are AAC64488, AAC64487, and CDG76955, respectively. The GenBank accession numbers of the corresponding codon-optimized *phzE*, *phzD* and *dhbX* genes are OK275489, OK275488, and OK275490, respectively.

3. Results

3.1. Functional Expression of the C3N Pathway Genes in *S. cerevisiae*

As aforementioned, three enzymes that can convert chorismate to 3-HAA are needed for building the short detour NAD biosynthesis pathway in *S. cerevisiae*. The genes that encode the three enzymes of 2-amino-2-deoxyisochorismate (ADIC) synthase *PhzE*, 2,3-dihydro-3-hydroxyanthranilic acid (DHHA) synthase *PhzD*, and DHHA dehydrogenase *DhbX* are all from Gram-positive bacteria with high G + C genomes [31,32]. Therefore, the codon-optimized *phzE*, *phzD*, and *dhbX* genes were synthesized and inserted into pYES2.0 plasmid under the control of the constitutive *TEF1* promoter *P_{TEF1}*, and then introduced into wild *S. cerevisiae* BY4741 (BY00) to construct the individual gene expression strain *S. cerevisiae* BY00-*phzE*, BY00-*phzD*, and BY00-*dhbX*, respectively. The functions of those proteins were further verified by in vitro enzymatic reactions. It was shown that the crude proteins of *S. cerevisiae* BY00-*phzE* could convert chorismate to ADIC (Figure 2A); the mixture crude proteins of *S. cerevisiae* BY00-*phzE* and *S. cerevisiae* BY00-*phzD* could convert chorismate to DHHA together (Figure 2B), and the protein of *S. cerevisiae* BY00-*dhbX* could convert DHHA to 3-HAA (Figure 2C). Overall, the results suggested that the *phzE*, *phzD*, and *dhbX* genes could be used to build the shorter C3N pathway in *S. cerevisiae* to replace the native *de novo* NAD⁺ biosynthesis pathway II.

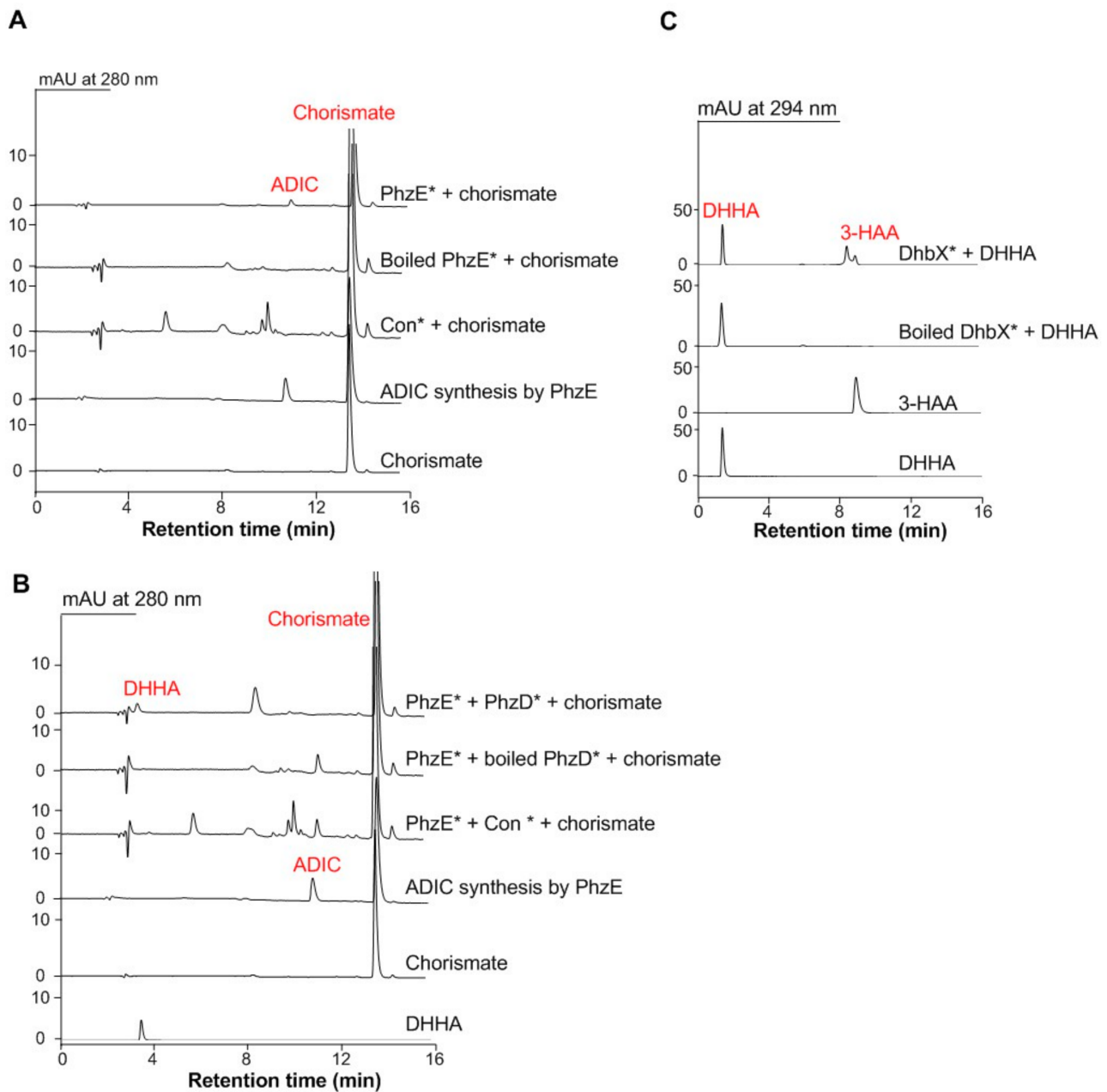


Figure 2. Representative assay of the C3N pathway enzymes in *S. cerevisiae*. **(A)** Representative enzymatic assays using the crude proteins of wild type *S. cerevisiae* BY00-pYES2.0 (Con*) and BY00-*phzE* (PhzE*). **(B)** Representative enzymatic assays using the crude proteins of wild type *S. cerevisiae* BY00-pYES2.0 (Con*), BY00-*phzD* (PhzD*), and BY00-*phzE* (PhzE*). **(C)** Representative enzymatic assays using the proteins of DhbX*.

3.2. Construction of the C3N Pathway in *S. cerevisiae*

To test the applicability of C3N pathway in *S. cerevisiae*, we constructed an NAD⁺ auxotrophic *S. cerevisiae* strain BY01 by knocking out the *BNA2* gene, which encodes a tryptophan 2,3-dioxygenase that catalyzes the first step of *de novo* NAD⁺ biosynthesis pathway II [33] (Figures 1 and 3A). As 3-HAA is not stable and tends to be oxidized in air, we used QA as a supplement and added to the YMMN solid medium for growth experiment. As anticipated, the wild-type strain *S. cerevisiae* BY00 could grow well on YMMN plate, whereas the NAD⁺ auxotrophic strain *S. cerevisiae* BY01 was unable to grow on YMMN plate unless QA was supplemented (Figure 3B). It suggested that the

pathway converting L-Trp to 3-HAA was blocked, whereas the enzymes responsible for the late steps of pathway II that converts 3-HAA to NAD⁺ are functionally expressed in *S. cerevisiae* BY01.

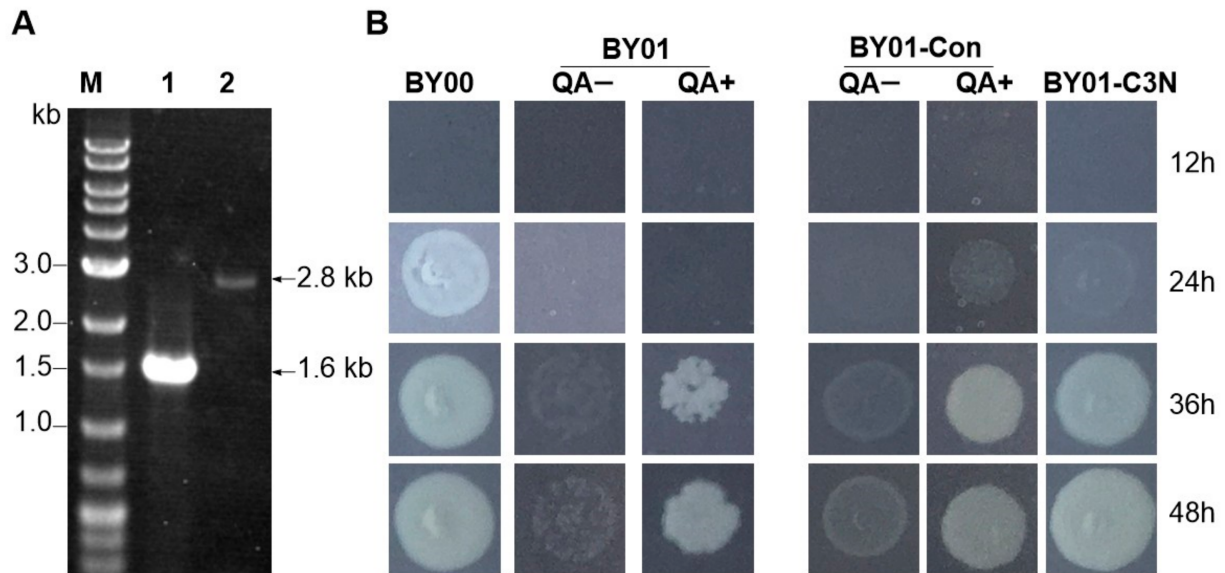


Figure 3. Verification of the C3N pathway applicability in *S. cerevisiae*. (A) Genotype verification of the NAD⁺ auxotrophic *S. cerevisiae* strain BY01, in which the tryptophan 2,3-dioxygenase *BNA2* was knocked out. Lane M, DNA marker; Lane 1 and lane 2 represent the PCR products of wild type *S. cerevisiae* BY00 and the $\Delta BNA2$ mutant BY01, respectively. (B) Growth of *S. cerevisiae* BY00 (wild type), the $\Delta BNA2$ mutant BY01, BY01-Con (control strain with empty vector), and BY01-C3N (with a complete C3N pathway) on YMMN plates with or without QA (10 mM) addition.

Subsequently, we constructed pY-C3N by sequentially cloning *phzE* and *phzD* into plasmid pYE-*P_{TEF1}-dhbX* and transformed the resultant plasmid pY-C3N into *S. cerevisiae* BY01 to generate *S. cerevisiae* BY01-C3N with a complete C3N pathway. A control strain *S. cerevisiae* BY01-Con was constructed by transforming the empty pYES2.0 plasmid into *S. cerevisiae* BY01. As anticipated, *S. cerevisiae* BY01, *S. cerevisiae* BY01-Con was unable to grow on YMMN plate without QA supplementation (Figure 3B). In contrast, *S. cerevisiae* BY01-C3N could grow well on YMMN plate without QA supplementation, indicating that the C3N pathway was successfully constructed in BY01-C3N and could synthesize NAD⁺ efficiently for its growth.

Subsequently, *S. cerevisiae* BY00, BY00-Con, BY01, BY01-Con, and BY01-C3N were cultivated in YMMN liquid medium for evaluating their growth. As anticipated, although slightly vague colony formed on solid plate with an initial OD₆₀₀ = 0.1, *S. cerevisiae* BY01 and BY01-Con were unable to grow in liquid YMMN medium without QA supplementation, as shown in Figure S1. Meanwhile, compared to the BY00 and BY00-Con exhibited normal growth curves, the mutant strain BY01-C3N displayed a clear growth delay (Figure 4A). Cellular NAD(H) levels of those strains were measured when the engineered strains reached early stationary phase. The cellular NAD(H) level of BY00-Con (2.92 ± 0.20 mM) was slightly lower than that of BY00 (3.30 ± 0.45 mM) (Table 1), indicating that the introduction of pYES2.0 had some influence on cell metabolism. The cellular NAD(H) level of BY01-C3N (3.13 ± 0.06 mM) was comparable to that of BY00 (Table 1), implying that the constructed C3N pathway is as efficient as the native *de novo* NAD⁺ biosynthesis pathway II in *S. cerevisiae*.

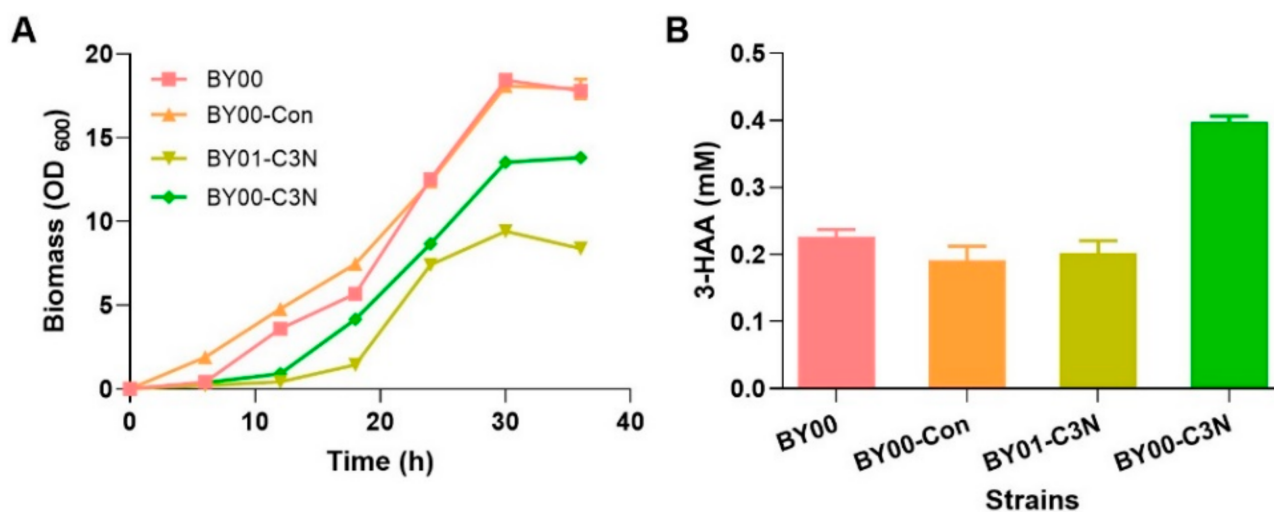


Figure 4. Comparison of the growth curves and the cellular 3-HAA concentrations of different *S. cerevisiae* strains. **(A)** The growth curves of *S. cerevisiae* BY00 (wild type), BY00-Con (wild type with empty vector), BY01-C3N ($\Delta BNA2$ mutant with a complete C3N pathway), and BY00-C3N (wild type with a complete C3N pathway) at 30 °C in YMMN medium with 20 g/L glucose addition. **(B)** The cellular 3-HAA concentrations of *S. cerevisiae* BY00-C3N and the control strains in 20 mL YMMN medium. Data presented as mean \pm SD, $n = 3$, and p -values were calculated using two-tailed t -tests.

Table 1. The cellular NAD(H) and NAD⁺ concentrations of different *S. cerevisiae* strains.

| Strains | NAD(H) [mM] | NAD ⁺ [mM] |
|----------|-----------------|-----------------------|
| BY00 | 3.30 \pm 0.45 | 1.90 \pm 0.24 |
| BY00-Con | 2.92 \pm 0.20 | 1.40 \pm 0.19 |
| BY01-C3N | 3.13 \pm 0.06 | 1.65 \pm 0.09 |
| BY00-C3N | 4.59 \pm 0.37 | 2.30 \pm 0.25 |

Note: The standard deviation (mean \pm SD) was calculated from independent triplicate biological experiments.

3.3. Expanding the NAD(H) Pool of *S. cerevisiae* by the C3N Pathway

To further explore cofactor engineering potency of the C3N pathway in *S. cerevisiae*, strain BY00-C3N was constructed by introducing the C3N module into *S. cerevisiae* BY00. In BY00-C3N, the key intermediate 3-HAA for NAD⁺ biosynthesis could be synthesized via both the C3N pathway that starts from chorismate and pathway II that starts from L-Trp (Figure 1). When cultivated in YMMN liquid medium, BY00-C3N displayed a similar growth deficiency phenomenon as BY01-C3N (Figure 4A), which may be caused by the metabolic burden of the C3N module overexpression. Analysis of the cellular metabolites revealed that an excess amount of 3-HAA (0.40 \pm 0.01 mM) was accumulated in BY00-C3N compared to the other three *S. cerevisiae* strains (BY00, BY00-Con, and BY01-C3N), in which 3-HAA was accumulated at nearly a half level (Figure 4B), no other metabolites were identified by HPLC. The cellular NAD(H) level of BY00-C3N reached 4.59 \pm 0.37 mM, which was about 40% higher than that of BY00 (Table 1), suggesting that the C3N pathway has a potential to elevate the cellular level of NAD(H) in *S. cerevisiae*.

4. Discussion

NAD⁺ is a life-essential metabolite involved in numerous redox reactions and multiple cellular physiological processes. Since it was discovered as the first ‘cozymase’ more than 100 years ago, two natural *de novo* NAD⁺ biosynthetic pathways (pathway I and II) have been elucidated and both of them start from a proteinogenic amino acid [4,9]. In a previous study, we designed an alternative *de novo* NAD⁺ biosynthesis pathway, the C3N pathway that starts from chorismate, and established this pathway successfully in *E. coli* by expressing four exogenous genes encoding an ADIC synthase, a DHHA synthase, a

DHHA dehydrogenase, and a 3-HAA 3,4-dioxygenase [16]. Chorismate can be converted to 3-HAA by the former three enzymes, and then undergo the oxidative ring cleavage catalyzed by 3-HAA 3,4-dioxygenase and a spontaneous cyclization to form QA, which will enter the native *de novo* NAD⁺ biosynthetic pathway I of *E. coli* and generate NAD⁺ via three steps common to all *de novo* NAD⁺ biosynthetic pathways [9,16]. Our previous work demonstrated the advantages of the C3N pathway in prokaryotic cells. In this study, we showed that the C3N pathway is also applicable in eukaryotic cells using *S. cerevisiae* as a model system. *S. cerevisiae* synthesizes NAD⁺ via *de novo* NAD⁺ biosynthetic pathway II, which also recruits 3-HAA 3,4-dioxygenase to convert 3-HAA to QA [17]. Therefore, only ADIC synthase, DHHA synthase, and DHHA dehydrogenase are necessary to build the C3N pathway in *S. cerevisiae*. The biosynthesis of NAD⁺ in *S. cerevisiae* BY01, a mutant strain deficient in synthesizing 3-HAA, could be restored to a normal level by introducing the C3N module, presenting the first example of eukaryotic cells that can survive on the artificial C3N pathway. Compared to the native chorismate to 3-HAA process composed of nine steps in yeast, only three steps are needed in the short detour of the C3N pathway [21].

It was shown that the C3N pathway could increase the cellular NAD(H) concentration more than nine times to about 9.3 mM in *E. coli* [16]. To explore the cofactor engineering potency of the C3N pathway in *S. cerevisiae*, the genes of C3N pathway were introduced to *S. cerevisiae* wild-type strain to generate BY00-C3N, in which the native *de novo* NAD⁺ biosynthesis pathway II is effective, and the build-in C3N module will supply extra amount of 3-HAA. As anticipated, the cellular NAD(H) level of BY00-C3N was considerably higher than that of BY00-Con or BY00, identifying its applicability in cofactor engineering in eukaryotic cells. However, it was not as effective as using the C3N module for cellular NAD(H) level improvement in *E. coli*. One possible reason is that the three C3N module enzymes from bacteria were not expressed well in *S. cerevisiae*. As shown in Figure 2, we could observe a poorly catalytic ability of the enzymes PhzE and PhzD expressed into *S. cerevisiae*. Meanwhile, the naturally competing metabolic pathways of chorismate may be other reasons that caused the ineffectiveness of the C3N pathway. Moreover, metabolic profile analysis of BY00-C3N revealed that more 3-HAA was accumulated compared to the other engineered strains, revealing that the 3-HAA 3,4-dioxygenase from pathway II could not convert the extra 3-HAA synthesized by the C3N module to QA efficiently [21]. Those work pave a way for further improvement of the cellular NAD(H) levels in yeast.

As a product of the shikimate pathway, chorismate is a natural branch point for various metabolic pathways [34–36]. It is abundant in many different cells including bacteria, archaea, fungi, and plants [37]. Therefore, the C3N pathway has the potential to be used in diverse organisms. Here, we showed that, in addition to the prokaryotic *E. coli* cells, the C3N pathway could supply NAD⁺ efficiently in the eukaryotic yeast cells via a more economical short detour, which set the stage for the application of this pathway in the other eukaryotes like fungi and plants.

Supplementary Materials: The following supporting information can be downloaded at: <https://www.mdpi.com/article/10.3390/fermentation9100886/s1>, Figure S1: The growth phenotypes of different engineered *S. cerevisiae* in YMMN medium. Table S1: Strains and plasmids used in this study.

Author Contributions: Conceptualization, X.L. and Y.C.; methodology, X.L., Y.T. and Y.D.; validation, X.L., Y.T. and P.L.; investigation, X.L. and Y.D.; Writing—Original draft preparation, X.L.; Writing—Review and editing, X.L., Y.T. and Y.C.; supervision, P.L. and Y.C.; funding acquisition, Y.C. All authors have read and agreed to the published version of the manuscript.

Funding: This work was supported in part by in part by the National Key R&D Program of China (2018YFA0901600), the National Natural Science Foundation of China (32370058 and 32025002), and the Transformation Program of S&T Achievements of Inner Mongolia (2020CG0012).

Institutional Review Board Statement: Not applicable.

Informed Consent Statement: Not applicable.

Data Availability Statement: The data that support the findings of this study are available from the corresponding author upon reasonable request.

Conflicts of Interest: The authors declare no competing interests.

References

1. Selles, V.L.; Kelly, C.L.; Mordaka, P.M.; Heap, J.T. Review of NAD(P)H-dependent oxidoreductases: Properties, engineering and application. *Biochim. Et Biophys. Acta (BBA) Proteins Proteom.* **2018**, *1866*, 327–347. [[CrossRef](#)] [[PubMed](#)]
2. Covarrubias, A.J.; Perrone, R.; Grozio, A.; Verdin, E. NAD⁺ metabolism and its roles in cellular processes during ageing. *Nat. Rev. Mol. Cell Biol.* **2021**, *22*, 119–141. [[CrossRef](#)] [[PubMed](#)]
3. Wang, M.; Chen, B.; Fang, Y.; Tan, T. Cofactor engineering for more efficient production of chemicals and biofuels. *Biotechnol. Adv.* **2017**, *35*, 1032–1039. [[CrossRef](#)] [[PubMed](#)]
4. Ying, W. NAD⁺/NADH and NADP⁺/NADPH in cellular functions and cell death: Regulation and biological consequences. *Antioxid. Redox Signal.* **2018**, *10*, 179–206. [[CrossRef](#)] [[PubMed](#)]
5. Katsyuba, E.; Auwerx, J. Modulating NAD⁺ metabolism, from bench to bedside. *EMBO J.* **2017**, *36*, 2670–2683. [[CrossRef](#)] [[PubMed](#)]
6. Zhou, Y.J.; Yang, W.; Wang, L.; Zhu, Z.; Zhang, S.; Zhao, Z.K. Engineering NAD⁺ availability for *Escherichia coli* whole-cell biocatalysis: A case study for dihydroxyacetone production. *Microb. Cell Factories* **2013**, *12*, 103. [[CrossRef](#)]
7. Li, F.; Li, Y.; Cao, Y.; Wang, L.; Liu, C.; Shi, L.; Song, H. Modular engineering to increase intracellular NAD(H⁺) promotes rate of extracellular electron transfer of *Shewanella oneidensis*. *Nat. Commun.* **2018**, *9*, 3637. [[CrossRef](#)] [[PubMed](#)]
8. Liu, J.; Li, H.; Zhao, G.; Caiyin, Q.; Qiao, J. Redox cofactor engineering in industrial microorganisms: Strategies, recent applications and future directions. *J. Ind. Microbiol. Biotechnol.* **2018**, *45*, 313–327. [[CrossRef](#)]
9. Sharma, S.; Hsieh, Y.-C.; Dietze, J.; Bockwolfdt, M.; Strömland, Ø.; Ziegler, M.; Heiland, I. Early Evolutionary Selection of NAD Biosynthesis Pathway in Bacteria. *Metabolites* **2022**, *12*, 569. [[CrossRef](#)]
10. Heuser, F.; Schroer, K.; Lütz, S.; Bringer-Meyer, S.; Sahm, H. Enhancement of the NAD(P)H pool in *Escherichia coli* for biotransformation. *Eng. Life Sci.* **2007**, *7*, 343–353. [[CrossRef](#)]
11. Katoh, A.; Uenohara, K.; Akita, M.; Hashimoto, T. Early steps in the biosynthesis of NAD⁺ in *Arabidopsis* start with aspartate and occur in the plastid. *Plant Physiol.* **2006**, *141*, 851–857. [[CrossRef](#)] [[PubMed](#)]
12. Kurnasov, O.; Goral, V.; Colabroy, K.; Gerdes, S.; Anantha, S.; Osterman, A.; Begley, T.P. NAD biosynthesis: Identification of the tryptophan to quinolinate pathway in bacteria. *Chem. Biol.* **2003**, *10*, 1195–1204. [[CrossRef](#)] [[PubMed](#)]
13. Rodionov, D.A.; De Ingeniis, J.; Mancini, C.; Cimadamore, F.; Zhang, H.; Osterman, A.L.; Raffaelli, N. Transcriptional regulation of NAD⁺ metabolism in bacteria: NrtR family of Nudix-related regulators. *Nucleic Acids Res.* **2008**, *36*, 2047–2059. [[CrossRef](#)] [[PubMed](#)]
14. Malkowski, S.N.; Spencer, T.C.J.; Breaker, R.R. Evidence that the *nadA* motif is a bacterial riboswitch for the ubiquitous enzyme cofactor NAD⁺. *RNA* **2019**, *25*, 1616–1627. [[CrossRef](#)] [[PubMed](#)]
15. Croft, T.; Venkatakrisnan, P.; Raj, C.J.T.; Groth, B.; Cater, T.; Salemi, M.R.; Phinney, B.; Lin, S.J. N-terminal protein acetylation by NatB modulates the levels of Nmnats, the NAD⁺ biosynthetic enzymes in *Saccharomyces cerevisiae*. *J. Biol. Chem.* **2020**, *295*, 7362–7375. [[CrossRef](#)] [[PubMed](#)]
16. Ding, Y.; Li, X.L.; Horsman, G.P.; Li, P.W.; Wang, M.; Li, J.E.; Zhang, Z.; Liu, W.; Wu, B.; Tao, Y.; et al. Construction of an alternative NAD⁺ *de novo* biosynthesis pathway. *Adv. Sci.* **2021**, *8*, 2004632. [[CrossRef](#)] [[PubMed](#)]
17. Wang, Y.; Liu, K.; Yang, Y.; Davis, I.; Liu, A. Observing 3-hydroxyanthranilate-3,4-dioxygenase in action through a crystalline lens. *Proc. Natl. Acad. Sci. USA* **2020**, *117*, 19720–19730. [[CrossRef](#)]
18. Hammer, S.K.; Avalos, J.L. Harnessing yeast organelles for metabolic engineering. *Nat. Chem. Biol.* **2017**, *13*, 823–832. [[CrossRef](#)]
19. Chen, R.E.; Thorner, J. Function and regulation in MAPK signaling pathways: Lessons learned from the yeast *Saccharomyces cerevisiae*. *Biochim. Biophys. Acta* **2007**, *1773*, 1311–1340. [[CrossRef](#)]
20. Gershon, H.; Gershon, D. The budding yeast, *Saccharomyces cerevisiae*, as a model for aging research: A critical review. *Mech. Ageing Dev.* **2000**, *120*, 1–22. [[CrossRef](#)]
21. Raj, C.J.T.; Lin, S.J. Cross-talk in NAD⁺ metabolism: Insights from *Saccharomyces cerevisiae*. *Curr. Genet.* **2019**, *65*, 1113–1119.
22. Oliveira, A.P.; Ludwig, C.; Zampieri, M.; Weisser, H.; Aebersold, R.; Sauer, U. Dynamic phosphoproteomics reveals TORC1-dependent regulation of yeast nucleotide and amino acid biosynthesis. *Sci. Signal.* **2015**, *8*, rs4. [[CrossRef](#)] [[PubMed](#)]
23. Gietz, R.D.; Schiestl, R.H. High-efficiency yeast transformation using the LiAc/SS carrier DNA/PEG method. *Nat. Protoc.* **2017**, *2*, 31–34. [[CrossRef](#)] [[PubMed](#)]
24. Inoue, H.; Nojima, H.; Okayama, H. High efficiency transformation of *Escherichia coli* with plasmids. *Gene* **1990**, *96*, 23–28. [[CrossRef](#)] [[PubMed](#)]
25. Hao, T.; Xie, Z.; Wang, M.; Liu, L.; Zhang, Y.; Wang, W.; Zhang, Z.; Zhao, X.; Li, P.; Guo, Z.; et al. An anaerobic bacterium host system for heterologous expression of natural product biosynthetic gene clusters. *Nat. Commun.* **2019**, *10*, 3665. [[CrossRef](#)] [[PubMed](#)]
26. Li, P.; Chen, M.; Tang, W.; Guo, Z.; Zhang, Y.; Wang, M.; Horsman, G.P.; Zhong, J.; Lu, Z.; Chen, Y. Initiating polyketide biosynthesis by on-line methyl esterification. *Nat. Commun.* **2021**, *12*, 4499. [[CrossRef](#)]

27. Kern, S.E.; Price-Whelan, A.; Newman, D.K. Extraction and measurement of NAD(P)⁺ and NAD(P)H. In *Pseudomonas Methods and Protocols*; Filloux, A., Ramos, J.L., Eds.; Humana Press: New York, NY, USA, 2014; pp. 311–323.
28. Day, A.; Schneider, C.; Schneider, B.L. Yeast Cell Synchronization. In *Cell Cycle Checkpoint Control Protocols*; Lieberman, H., Ed.; Humana Press: New York, NY, USA, 2004; pp. 55–76.
29. Sporty, J.; Lin, S.J.; Kato, M.; Ognibene, T.; Stewart, B.; Turteltaub, K.; Bench, G. Quantitation of NAD⁺ biosynthesis from the salvage pathway in *Saccharomyces cerevisiae*. *Yeast* **2009**, *26*, 363–369. [[CrossRef](#)]
30. Tang, W.; Guo, Z.; Cao, Z.; Wang, M.; Li, P.; Meng, X.; Zhao, X.; Xie, Z.; Wang, W.; Zhou, A.; et al. D-Sedoheptulose-7-phosphate is a common precursor for the heptoses of septacidin and hygromycin B. *Proc. Natl. Acad. Sci. USA* **2018**, *115*, 2818–2823. [[CrossRef](#)]
31. Culbertson, J.E.; Toney, M.D. Expression and characterization of PhzE from *P. aeruginosa* PAO1: Aminodeoxyisochorismate synthase involved in pyocyanin and phenazine-1-carboxylate production. *Biochim. Biophys. Acta* **2013**, *183*, 240–246. [[CrossRef](#)]
32. Parsons, J.F.; Calabrese, K.; Eisenstein, E.; Ladner, J.E. Structure and mechanism of *Pseudomonas aeruginosa* PhzD, an isochorismatase from the phenazine biosynthetic pathway. *Biochemistry* **2003**, *42*, 5684–5693. [[CrossRef](#)]
33. Iwamoto, Y.; Lee, I.S.; Tsubaki, M.; Kido, R. Tryptophan 2,3-dioxygenase in *Saccharomyces cerevisiae*. *Can. J. Microbiol.* **1995**, *41*, 19–26. [[CrossRef](#)]
34. Almeida, A.M.; Marchiosi, R.; Abrahão, J.; Constantin, R.P.; dos Santos, W.D.; Ferrarese-Filho, O. Revisiting the shikimate pathway and highlighting their enzyme inhibitors. *Phytochem. Rev.* **2023**, 1–37. [[CrossRef](#)]
35. Lynch, J.H.; Dudareva, N. Aromatic amino acids: A complex network ripe for future exploration. *Trends Plant Sci.* **2020**, *25*, 670–681. [[CrossRef](#)]
36. Hubrich, F.; Müller, M.; Andexer, J.N. Chorismate- and isochorismate converting enzymes: Versatile catalysts acting on an important metabolic node. *Chem. Commun.* **2021**, *57*, 2441–2463. [[CrossRef](#)]
37. Wu, S.; Chen, W.; Lu, S.; Zhang, H.; Yin, L. Metabolic engineering of shikimic acid biosynthesis pathway for the production of shikimic acid and its branched products in microorganisms: Advances and Prospects. *Molecules* **2022**, *27*, 4779. [[CrossRef](#)]

Disclaimer/Publisher’s Note: The statements, opinions and data contained in all publications are solely those of the individual author(s) and contributor(s) and not of MDPI and/or the editor(s). MDPI and/or the editor(s) disclaim responsibility for any injury to people or property resulting from any ideas, methods, instructions or products referred to in the content.